Electrospinning of polymer nanofibres from multiple jets on a porous tubular surface

2006 Nanotechnology 17 1123

(http://iopscience.iop.org/0957-4484/17/4/046)

INSTITUTE OF PHYSICS PUBLISHING NANOTECHNOLOGY
Nanotechnology **17** (2006) 1123–1127 doi:10.1088/0957-4484/17/4/046

Electrospinning of polymer nanofibres from multiple jets on a porous tubular surface

O O Dosunmu[1], G G Chase[2,4], W Kataphinan[3] and D H Reneker[3]

[1] Department of Chemical Engineering, University of Lagos, Lagos, Nigeria
[2] Microscale Physiochemical Engineering Center, The University of Akron, Akron, OH 44325, USA
[3] Maurice Morton Institute of Polymer Science, The University of Akron, Akron, OH 44325, USA

E-mail: gchase@uakron.edu

Received 16 September 2005, in final form 19 December 2005
Published 2 February 2006
Online at stacks.iop.org/Nano/17/1123

Abstract
A novel method for the electrospinning of multiple polymer jets into nanofibres is presented. In this work, 20 wt% nylon 6 solution was electrified and pushed by air pressure through the walls of a porous polyethylene tube. Multiple jets formed on the porous surface and electrospun into nanoscale fibres. The length weighted fibre diameters have a similar mean diameter to those from a single jet but broader in distribution. The mass production rate from the porous tube is 250 times greater than from a typical single jet.

(Some figures in this article are in colour only in the electronic version)

1. Introduction

Production of nanofibres by electrospinning polymeric materials has attracted much attention. The remarkably large length to diameter ratio drives the interest. Electrospinning was introduced by Formhals in 1934 [1] and interest in the method grew rapidly in the 1990s.

Reneker [2] demonstrated the fabrication of ultra-thin fibres from a broad range of organic polymers. Li and Xia [3] recently published an extensive survey of advances in the electrospinning of nanofibres and potential applications. The applications of the nanostructures include filter media, composite materials, biomedical applications (tissue engineering, scaffolds, bandages and drug release systems), protective clothing, micro- and optoelectronic devices, photonic crystals and flexible photocells. For example, nanofibres provide significant increases in filtration efficiency of submicron particles [4]. Nanofibres improve separation efficiency in coalescence filtration for water in oil emulsions and in aerosol coalescence [5, 6].

In electrospinning, electrical forces produce a uniaxial stretching of a viscoelastic jet derived from a polymer solution or melt. The process uses an electric field to draw a polymer solution from the tip of a capillary. A high voltage is applied to the polymer solution (or melt), which causes the jet of solution to elongate as the jet is drawn toward a grounded collector. The jet undergoes an electrically induced bending instability which results in looping and accommodates great elongation of the jet [7–9]. The fine jet dries as the solvent evaporates, to form solid fibres with diameters in the submicron range.

The viscoelastic jets are customarily derived from drops that are suspended at the tip of a hollow metal needle, which is attached to a vessel filled with polymer solution. This arrangement typically produces a single jet and the mass rate of fibre deposition from a single jet is typically 0.1–1.0 g h^{-1}. To significantly increase the production rate of this design many jets are required. A multi-needle arrangement is often inconvenient due to its complexity and its high probability of clogging. Multiple jets were produced using a ferromagnetic fluid layer beneath a layer of polymer solution [10]. A magnetic field caused the interface to develop sharp peaks. Yarin and Zussman reported the possibility of a 12-fold increase in production rate over a comparable multi-needle arrangement. Jirsak *et al* [11] describe a rotating drum device for electrospinning multiple jets at a rate of about 1.5 g min^{-1} per meter length.

[4] Author to whom any correspondence should be addressed.

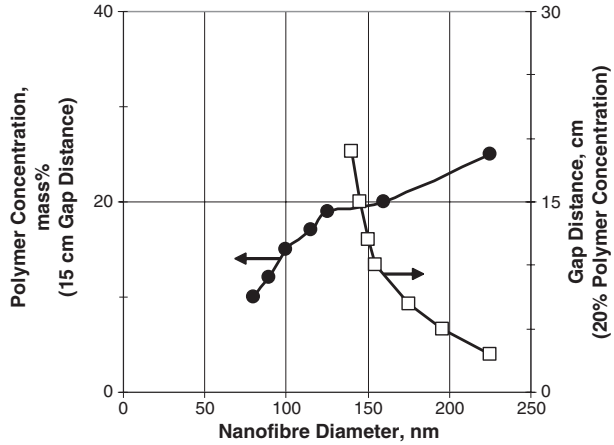

Figure 1. Variation in the average diameter of nylon 6 fibres electrospun from a single jet as a function of polymer concentration and gap distance [12].

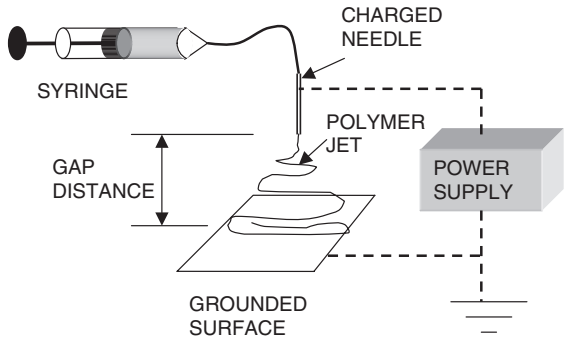

Figure 2. Diagram of hollow needle single-jet electrospinning apparatus. The polymer in the syringe is pushed though a flexible tube to the metal needle. The needle is charged to high voltage by the power supply. A polymer jet is emitted from a drop at the tip of the needle toward the grounded surface. The jet elongates and reduces in diameter, the solvent evaporates from the jet, and solid fibres are collected on the grounded surface.

In this paper fibres electrospun from a single syringe needle (as a single jet) are compared to fibres produced from multiple jets from a porous tube. Most literature only reports the average fibre diameter. In this paper we report the length weighted fibre diameter distribution as measured from multiple images of the fibre mats.

2. Single-jet hollow needle apparatus

Electrospun fibre diameters can vary from less than 100 nm to greater than 1000 nm, depending on the polymer, solvent, and operating conditions. To some degree the fibre diameters can be controlled by adjusting solvent concentration and gap distance, while holding other parameters constant. This is shown in figure 1.

The fibres reported in figure 1 were produced from a single jet emitted from a drop on the tip of a charged syringe needle as sketched in figure 2. Nylon 6 pellets (molecular weight 244, Sigma Aldrich CAS 25038-54-4) were dissolved in formic acid (Fisher Scientific CAS 64-18-6). The syringe pump was operated at a rate sufficient to maintain a liquid drop at the tip of the 0.5 mm ID metallic syringe needle (about 4 μl min^{-1}). The needle was charged to 20 000 V. The gap distance between the tip of the needle and the grounded surface in figure 2 was varied from 3 to 19 cm while the solution concentration was varied from 10 to 25 mass% nylon 6.

3. Multiple-jet porous tube apparatus

To produce fibres from multiple jets a porous walled cylindrical tube was filled with the polymer solution. The polymer was pushed through the pores to form drops on the outer surface of the tube. When the solution was charged, jets issued from the drops and formed many electrospun fibres.

Figure 3 shows a sketch of the experimental set-up with the porous tube. The tube axis was positioned vertically and was surrounded by a co-axial wire mesh grounded collector. A wire electrode was inserted into the bottom of the tube to charge the polymer solution. The top of the tube was equipped with fittings to connect to a pressurized air supply.

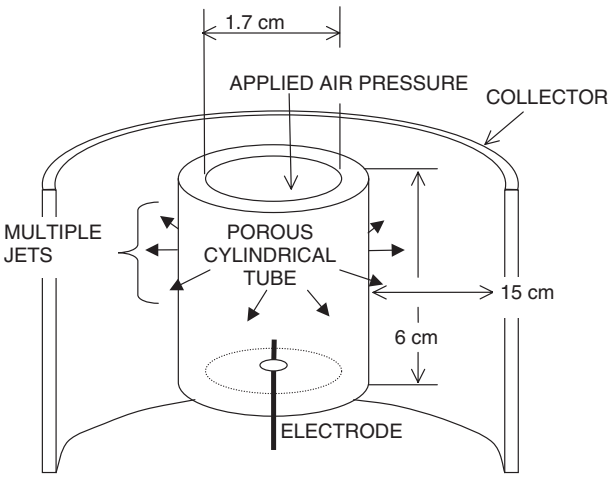

Figure 3. Cutaway view showing the cylindrical porous tube with its axis oriented vertically within a coaxial cylindrical collector (not to scale).

The pressurized air (0.4–0.8 kPa) provided sufficient force to push the polymer solution through the tube wall to feed or replace drops on the outer surface as the jets carry the solution away.

The porous tube, shown in figure 4, was machined from a solid porous polyethylene rod (GenPore, Reading, PA, USA). The tube had an internal diameter of 1.7 cm and external diameter of 3.1 cm, with one end permanently sealed. The camera lens was positioned to view the tube through one of the openings in the wire mesh. Some of the 20 wt% nylon polymer solution jets are indicated on the photograph.

The porous tube process can work with other tube materials and polymers. As an example figure 5 shows a ceramic tube and jets of polyvinylpyrrolidone (PVP, Aldrich, CAS 9003-39-8) in ethanol solution. In this experiment the PVP formed much larger and more visible jets and fibres than those shown in figure 4, though the processes are similar. The descriptions and the data analysis that follow are only for the nylon fibres produced by the tube shown in figure 4.

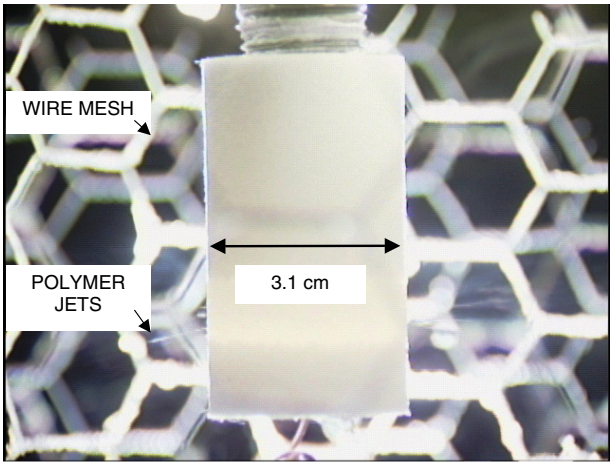

Figure 4. Photograph of jets from small drops on the tube surface. The jets elongate and dry into fibres that collect on the surrounding wire mesh. The wire mesh was constructed of hexagonal shaped holes roughly 3 cm in diameter. The camera is aimed through one of the holes in the mesh, hence the mesh in front of the tube is not visible.

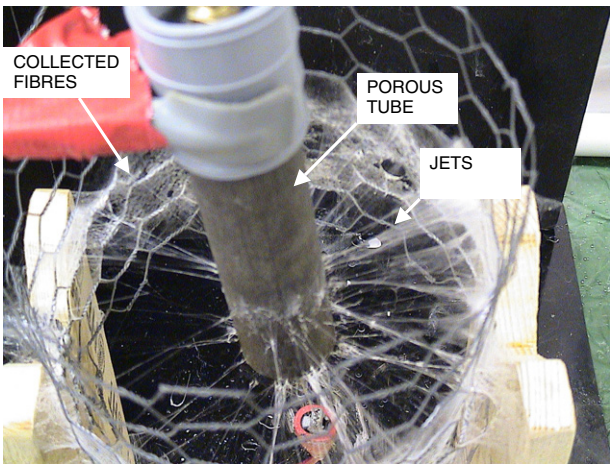

Figure 5. View from above of a ceramic porous tube and jets of polyvinylpyrrolidone (PVP) in ethanol solution spinning from the surface of the tube.

Figure 6 shows that the pores of the polyethylene tube wall in figure 4 are highly irregular. The pores vary in size from about 10 μm up to about 100 μm. The tube has a porosity of about 0.43 (volume of pores/volume of tube wall) and it has a Darcian permeability (inverse of resistance to flow) of the tube walls of about 2×10^{-9} m^2 (determined by flow of air).

The polymer solution flowed slowly through the porous wall and formed small drops on the outside surface. A variable high voltage power supply was used to charge the polymer solution to 20 000 V using the electrode inserted in the sealed end of the tube. The electric field caused jets to emit from the drops and move toward the collector surface. Many of the jets removed polymer from the drop faster than the polymer flowed through the porous wall. As the drops diminished in size some of the jets stopped but new jets formed on other, larger drops.

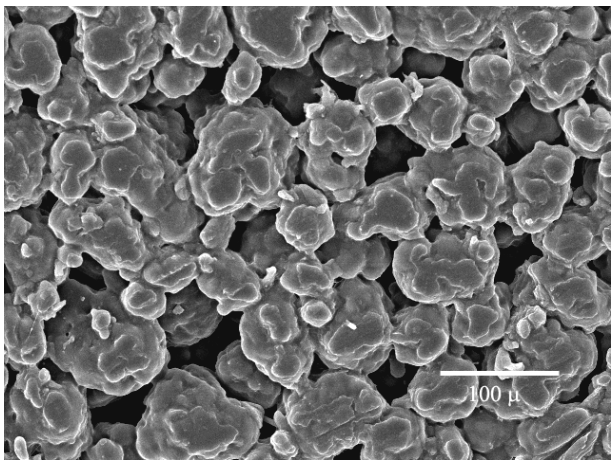

Figure 6. SEM image of the pores of the polyethylene tube walls. The wall is made of particles roughly 10–100 μm in size. The pores between these particles are highly irregular in shape and roughly 10–100 μm in size.

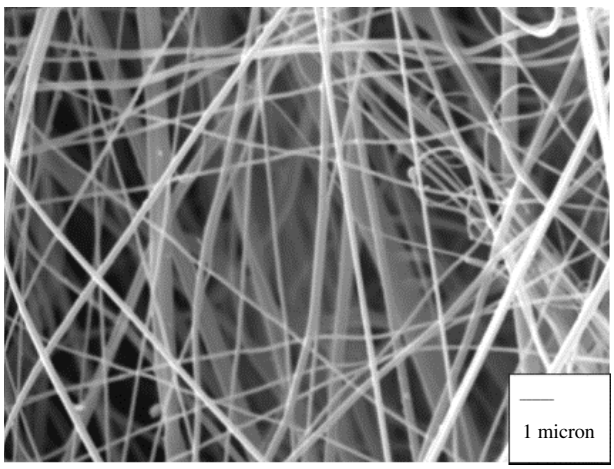

Figure 7. SEM image of nylon 6 fibres electrospun from the porous tube.

4. Experimental results and discussion

Figure 7 is a sample SEM image of fibres collected on the wire mesh surrounding the porous tube. IMAGEJ [13] image analysis software was used to determine the dimension of the fibres. The segments shown in the images are parts of very long fibres. The fibre diameters and segment lengths were measured from multiple SEM images. The size distributions are fitted to the Gaussian normal distribution and the log normal distribution functions.

The mean diameters and standard deviations for the normal and log-normal distributions were calculated using the expressions

$$\overline{x} = \frac{1}{L_{\text{tot}}} \sum L_i x_i \tag{1}$$

$$\sigma = \sqrt{\frac{\sum (L_i (x_i - \overline{x})^2)}{L_{\text{tot}}}} \tag{2}$$

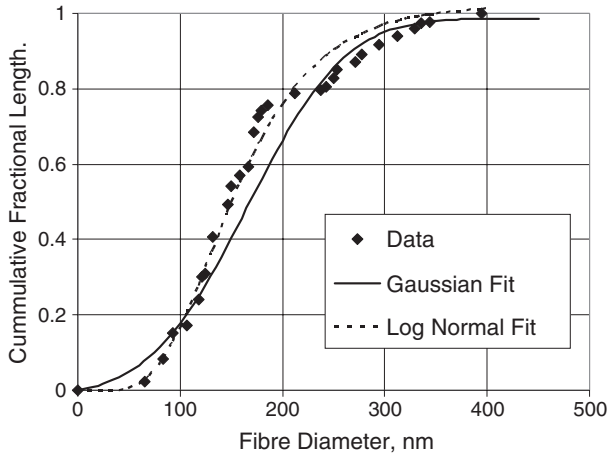

Figure 8. Fiber diameter cumulative distribution of nylon 6 made by electrospinning multiple jets from the porous tube. The data are compared with the normal and log-normal fitted curves.

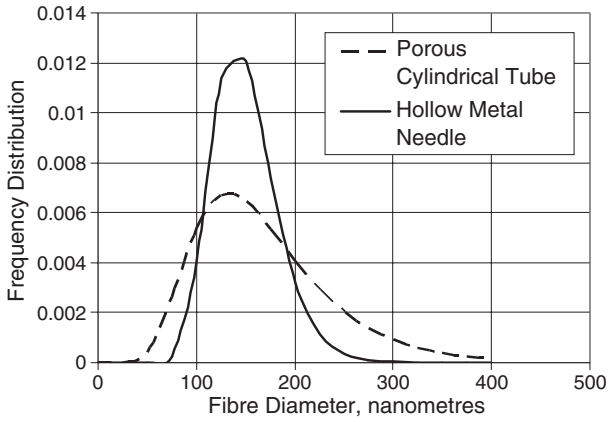

Figure 9. Length weighted log-normal frequency distributions of fibre diameters of nylon 6 electrospun from a single hollow metal needle and from the porous cylindrical tube.

$$\ln(\overline{x_g}) = \frac{1}{L_{tot}} \sum L_i \ln(x_i) \tag{3}$$

$$\ln(\sigma_g) = \sqrt{\frac{\sum (L_i (\ln(x_i) - \ln(\overline{x_g}))^2)}{L_{tot}}} \tag{4}$$

where $L_{tot} = \sum L_i$ and L_i is the length of the fibre segments of diameter x_i. The fitted parameters for the fibres from the porous tube are $\overline{x} = 170.6$ nm and $\sigma = 75.0$ for the Gaussian distribution and $\overline{x_g} = 156.4$ nm and $\sigma_g = 1.51$ for the log-normal distribution.

Plotted in figure 8 are the fitted diameter distributions and experimental data for fibres spun from the porous tube in figure 4. The log-normal distribution gives a better representation of the data than the normal distribution. This is confirmed by calculating the total area magnitudes between the fitted curves and the measured data. The total area of error between the normal distribution curve and the measured data has a magnitude of 17.5 nm whereas the area of error for the log-normal curve has a magnitude of 10.6 nm, showing the log-normal has the better fit.

Dimensions of fibres made from the hollow needle single-jet set-up were measured in a similar way. For these fibres the log-normal mean is $\overline{x_g} = 145.9$ nm and the standard deviation is $\sigma_g = 1.24$. The gap distance in figure 2 was 15 cm and 20 000 V were applied. The same polymer solution as used in the porous tube experiment was used in this experiment.

Figure 9 shows the frequency distribution plots of the fibre diameters obtained from the porous tube and the hollow needle. The distribution curves show a significant fraction of the fibres (on a length basis) have diameters less than 100 nm, but most of the fibres have diameters between 100 and 200 nm.

The comparison shows that the two distributions have similar mean diameters, but the distribution from the porous tube is broader than the distribution from the single jet. The exact reason for this is not clear but two mechanisms are plausible. First, the electric field acting on the drops on the surface of the porous tube has a different geometry than the electric field acting on the hollow needle. In the former case the field flux lines are directed radially from the tube surface to the collector surface, whereas in the latter case the field lines are strongly curved in the proximity of the drop on the tip of the needle.

Second, some of the jets such as those labelled in figure 4 appeared to have much larger diameters than others as they left the drops on the cylindrical surface. This may be due to some of the drops reaching a larger diameter than the drop on the tip of the hollow needle. A thicker initial jet normally produces larger diameter fibres. The drop size on the surface of the porous tube is influenced by the rate of polymer flow through the pores and by the strength of the electric field in the vicinity of the drop.

Smaller diameter fibres may be obtained by increasing the gap distance between the tube and collector surfaces in figure 3. The primary role of the pores in the tube wall is to provide a conduit for the polymer flow with a sufficient flow resistance that the polymer solution does not flow too rapidly and wet the outer tube surface with a liquid film.

The mass production rate of nanofibres from the porous tube was found to be very large compared to the single-needle arrangement. Some of this increased production rate is attributed to the larger fibre diameters, but most is attributed to the greater number of jets. Tens to hundreds of jets may emit from the tube surface at the same time. The exact number of jets is difficult to estimate because most of them are created and disappear in a short time. However, the combined production rate of all of these jets can be easily determined by weighing the fibres.

The single needle produced nanofibres at a rate of about 0.02 g h^{-1}. The 2 cm section of polymer filled porous tube used in this experiment produced nanofibres at a rate greater than 5 g h^{-1} or about 250 times the rate of the single needle. The porous tube is much simpler for construction, operation and control. It has potential for scale-up to long tube geometries. If the porous tube is linearly scaled, then the extrapolated production rate reaches the order of 4.2 g min^{-1} per meter length of tube.

5. Conclusions

We have demonstrated a device for electrospinning multiple jets from a cylindrical porous tube. The porous tube has a

significantly greater production rate over the single needle. Analysis of the fibres shows the fibre size distributions on a length weighted basis are similar in average size but the porous tube produces fibres with a broader distribution.

Acknowledgments

This work was supported by the Coalescence Filtration Nanomaterials Consortium: Ahlstrom Paper Group, Donaldson Company, Fleetguard, Hollingsworth and Vose, and Parker Hannifin. This work was also supported by the National Science Foundation grant number DMI-0403835.

References

[1] Formhals A 1934 *US Patent* 1,975,504
[2] Reneker D H and Chun I 1996 *Nanotechnology* **7** 216–23
[3] Li D and Xia Y 2004 *Adv. Mater.* **16** 1151–70
[4] Grafe T H and Graham K M 2003 Nanofiber webes form electrospinning *Presented at the Nonwovens in Filtration—5th Int. Conf. (Stuttgart, Germany, March 2003)*
[5] Shin C and Chase G G 2004 *AIChE J.* **50** 343–50
[6] Chase G G and Reneker D H 2004 *Fluid/Particle Separation J.* **16** 105–17
[7] Reneker D H, Yarin A L, Fong H and Koombhongse S 2000 *J. Appl. Phys.* **87** 4531
[8] Yarin A L, Koombhongse S and Reneker D H 2001 *J. Appl. Phys.* **89** 3018
[9] Hohman M M, Shin M, Rutledge G and Brenner M P 2001 *Phys. Fluids* **13** 2221
[10] Yarin A L and Zussman E 2004 *Polymer* **45** 2977–80
[11] Jirsak O, Sanetrnik F, Lukas D, Kotek V, Martinova L and Chaloupek J 2005 A method of nanofibres production from a polymer solution using electrostatic spinning and a device for carrying out the method PCT WO 2005/024101 A1
[12] Suthar A 2003 Nanofiber augmented meltblown filter media *MS Thesis* The University of Akron, Akron, Ohio
[13] Rasband W S 1997–2005 ImageJ, US National Institutes of Health, Bethesda, Maryland, USA(http://rsb.info.nih.gov/ij/)